Supplementary information

Defect Management by Cesium Fluoride-modified Electron Transport Layer Promotes Perovskite Solar Cells

Xiangning Xu,‡[a] Zhichao Lin,‡[a] Qingbin Cai,[a] Hongye Dong,[a] Xinli Wang[a] and Cheng Mu*[a]

a Key Laboratory of Advanced Light Conversion Materials and Biophotonics, Department of Chemistry Renmin University of China, Beijing, 100872, P. R. China.

Table S1. Band gap (E_g), secondary-electron cut-off ($E_{cut\text{-}off}$), Fermi level (E_F), valence band energy (E_{VB}), and conduction band energy (E_{CB}) of the original SnO_2 and the CsF-modified double-layer SnO_2 ETLs.

Sample	E_g (eV)	$E_{cut\text{-}off}$ (eV)	E_F (eV)	E_{VB} (eV)	E_{CB} (eV)
SnO_2	3.60	16.68	4.54	7.65	4.68
CsF-SnO_2	3.63	16.04	5.18	8.28	4.02

Table S2. Fitting parameters of TRPL spectra (excitation wavelength 475 nm) of perovskite films based on the original SnO_2 and the CsF-modified double-layer SnO_2 substrates.

Sample	A_1	τ_1 (ns)	A_2	τ_2 (ns)	τ_{AVE} (ns)
SnO_2	0.251	24.89	0.751	600.82	592.95
CsF-SnO_2	0.229	8.87	0.729	263.50	260.83

Table S3. Summary of the photovoltaic parameters of the PSCs based on different concentrations of ETLs.

Sample	V_{OC} (V)	J_{SC} (mA/cm^2)	FF	PCE (%)
SnO_2	1.114	23.00	0.763	19.80
0.5 mg/mL CsF-SnO_2	1.158	22.78	0.773	20.38

1.0 mg/mL CsF-SnO_2	1.159	23.27	0.778	20.98
2.0 mg/mL CsF-SnO_2	1.137	23.76	0.757	20.45

Table S4. V_{TFL} and N_t of the perovskite films based on original SnO_2 and CsF-modified double-layer SnO_2 ETLs.

Sample	L (nm)	ε	V_{TFL} (V)	N_t ($\times 10^{15}$ cm^{-3})
SnO_2	780	42.3	0.22	1.69
CsF-SnO_2	780	42.3	0.15	1.15

Table S5. The fitted parameters of the electrical impedance spectroscopy measurements under darkness of original and CsF-modified PSCs.

Samples	R_{rec} (Ω cm^2)
SnO_2	0.77×10^4
CsF-SnO_2	1.45×10^4

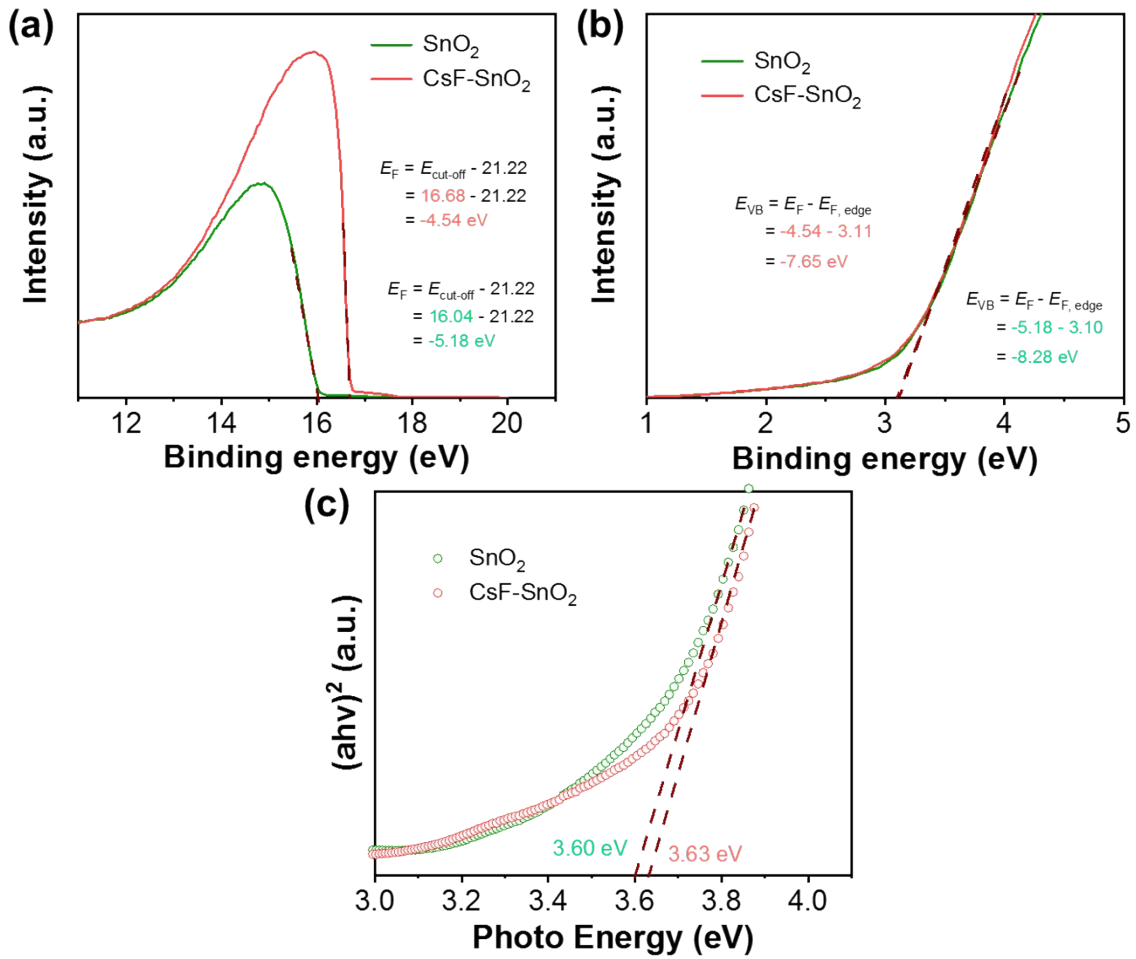

Fig. S1 (a), (b) ultraviolet photoelectron spectroscopy and c) ultraviolet-visible spectra of the original SnO_2 and CsF-modified double-layer SnO_2 films.

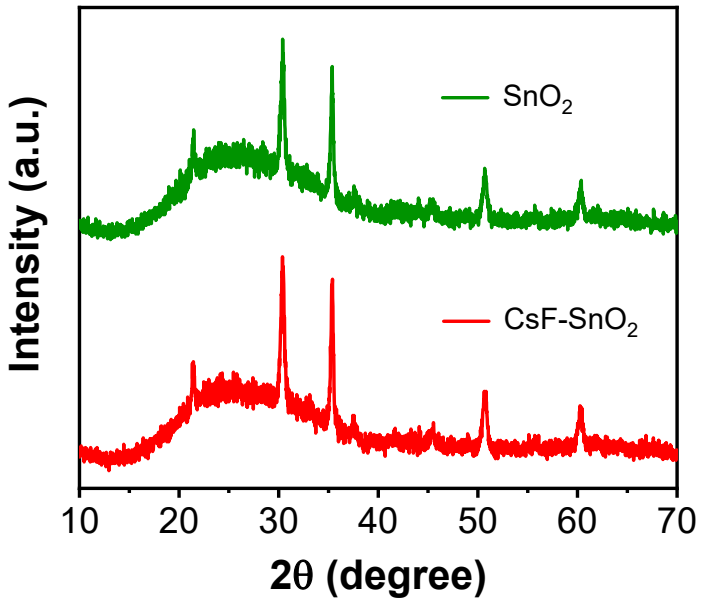

Fig. S2 X-ray diffraction patterns of the original SnO_2 and CsF-modified double-layer SnO_2 films.

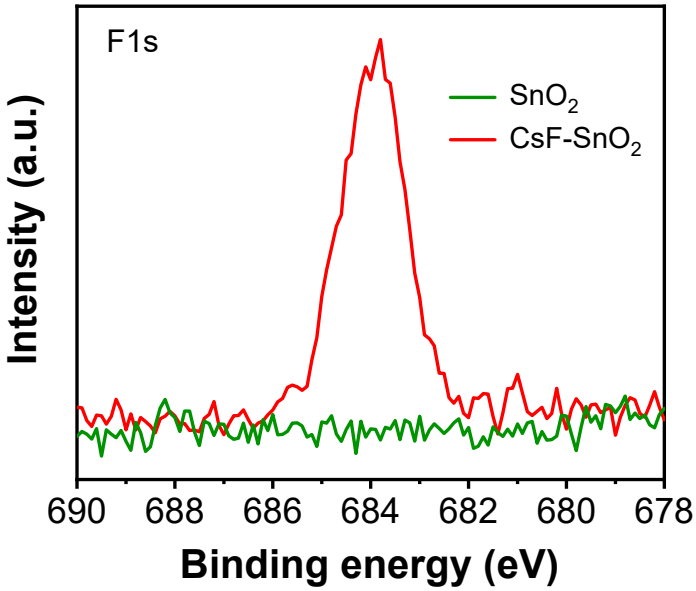

Fig. S3 High-resolution F 1s X-ray photoelectron spectroscopy spectra of the original SnO_2 and CsF-modified double-layer SnO_2 films.

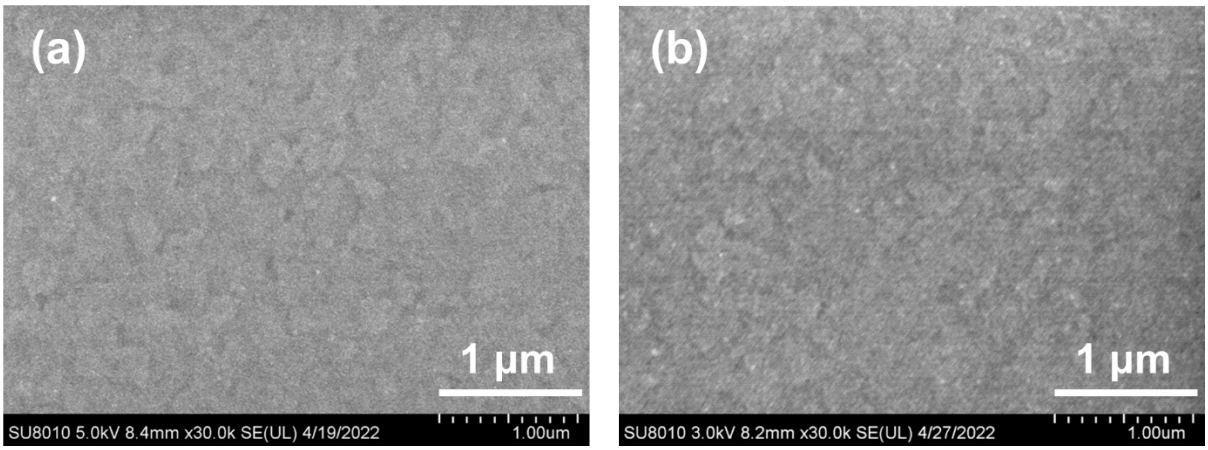

Fig. S4 Top view scanning electron microscopy images of (a) original SnO_2 and (b) CsF-modified double-layer SnO_2 films deposited on the ITO substrates.

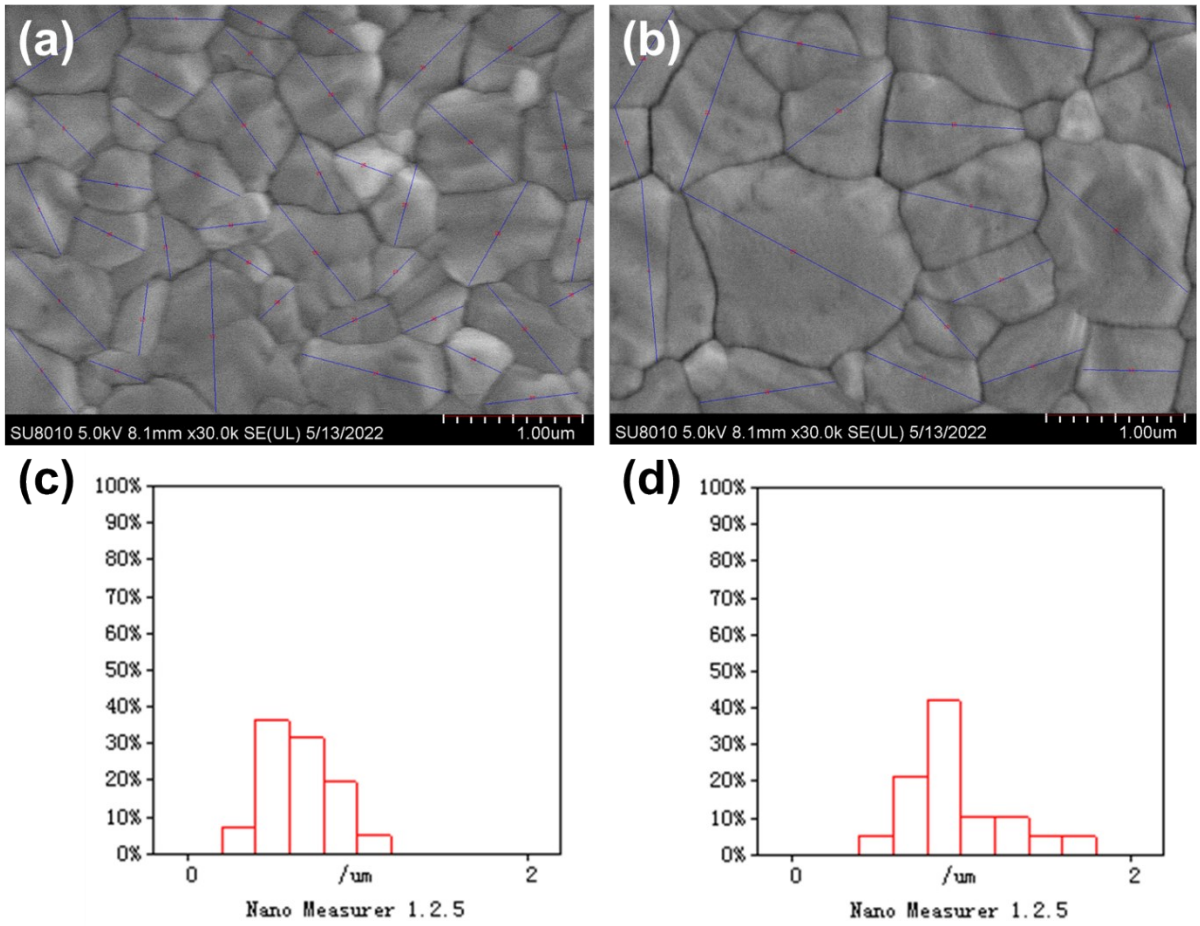

Fig. S5 Statistical distribution diagram of grain size of perovskite films deposited on the (a), (b) original SnO_2 and (c), (d) CsF-modified double-layer SnO_2 ETLs.

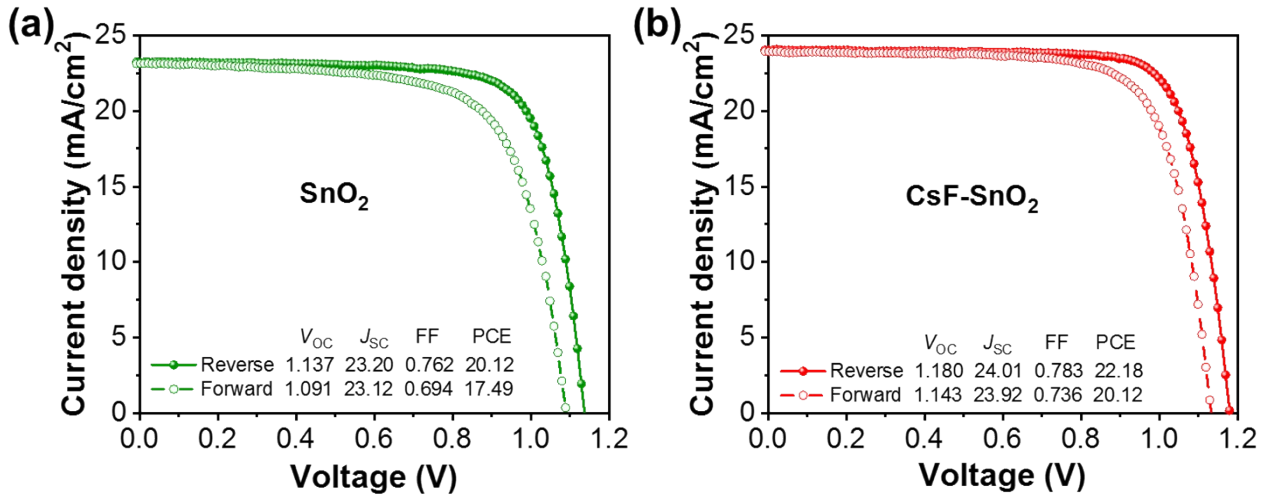

Fig. S6 *J–V* curves of the champion PSCs based on the (a) original SnO_2 and (b) CsF-modified double-layer SnO_2 ETLs.

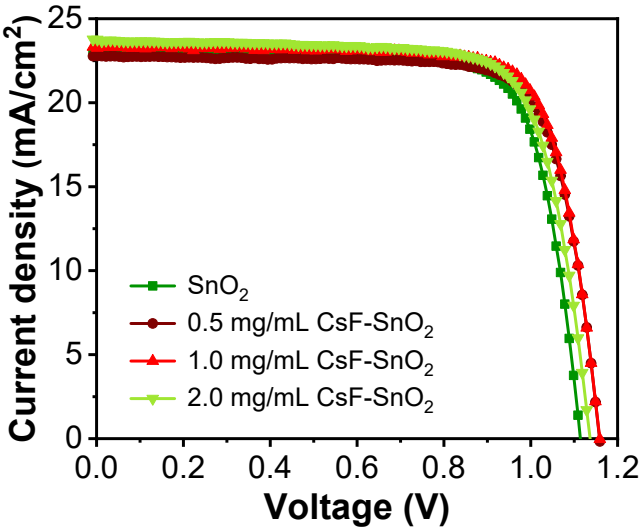

Fig. S7 *J–V* curves of the PSCs based on different concentrations of CsF-modified SnO_2 ETLs.